

## Endothelial Differentiation G Protein-Coupled Receptor 5 Plays an Important Role in Induction and Maintenance of Pluripotency

IRINA NEGANOVA,<sup>a</sup> LEWIS COTTS,<sup>a</sup> PETER BANKS,<sup>b</sup> KATJA GASSNER,<sup>a</sup> ANVAR SHUKUROV,<sup>c</sup>  
LYLE ARMSTRONG,<sup>a</sup> GRAHAM LADDS,<sup>d</sup> MAJLINDA LAKO <sup>a</sup>

**Key Words.** hESCs/hiPSCs • Human somatic cell reprogramming • Genome-wide RNAi screen • GPCR • EDG5 • Cytoskeleton

<sup>a</sup>International Centre for Life, Institute of Genetic Medicine, Newcastle University, Newcastle, United Kingdom;

<sup>b</sup>High Throughput Screening Facility, Medical School, Newcastle, United Kingdom;

<sup>c</sup>School of Mathematics and Statistics, Newcastle University, Newcastle upon Tyne, United Kingdom;

<sup>d</sup>Department of Pharmacology, University of Cambridge, Cambridge, United Kingdom

Correspondence: Majlinda Lako, Ph.D., International Centre for Life, Institute of Genetic Medicine, Newcastle University, Central Parkway, Newcastle NE1 3BZ, United Kingdom.  
Telephone: +44(0) 191 241 8688;  
e-mail: majlinda.lako@ncl.ac.uk

Received August 4, 2018; accepted for publication October 25, 2018; first published online in *STEM CELLS EXPRESS* December 4, 2018.

<http://dx.doi.org/10.1002/stem.2954>

This is an open access article under the terms of the Creative Commons Attribution License, which permits use, distribution and reproduction in any medium, provided the original work is properly cited.

### ABSTRACT

Direct reprogramming of human somatic cells toward induced pluripotent stem cells holds great promise for regenerative medicine and basic biology. We used a high-throughput small interfering RNA screening assay in the initiation phase of reprogramming for 784 genes belonging to kinase and phosphatase families and identified 68 repressors and 22 effectors. Six new candidates belonging to the family of the G protein-coupled receptors (GPCRs) were identified, suggesting an important role for this key signaling pathway during somatic cell-induced reprogramming. Downregulation of one of the key GPCR effectors, endothelial differentiation GPCR5 (EDG5), impacted the maintenance of pluripotency, actin cytoskeleton organization, colony integrity, and focal adhesions in human embryonic stem cells, which were associated with the alteration in the RhoA-ROCK-Cofilin-PAXILLIN-actin signaling pathway. Similarly, downregulation of EDG5 during the initiation stage of somatic cell-induced reprogramming resulted in alteration of cytoskeleton, loss of human-induced pluripotent stem cell colony integrity, and a significant reduction in partially and fully reprogrammed cells as well as the number of alkaline phosphatase positive colonies at the end of the reprogramming process. Together, these data point to an important role of EDG5 in the maintenance and acquisition of pluripotency. *STEM CELLS* 2019;37:318–331

### SIGNIFICANCE STATEMENT

Using a high-throughput RNA interference screen, authors identified 22 effectors of somatic cell-induced reprogramming, six of which belong to the G protein-coupled receptor (GPCR) family. The present study describes a new role for the GPCR family member, endothelial differentiation GPCR5 (EDG5; sphingosine-1-phosphate receptor 2), whose downregulation in human embryonic stem cells (hESCs) or during the initiation period of reprogramming leads to abrogation of the pluripotent stem cell colony formation because of the defects in cytoskeleton organization and focal adhesions. Together, the data provide for the first time substantive evidence for EDG5 as a critical GPCR for the maintenance of pluripotency in hESC and successful reprogramming of human fibroblasts to human-induced pluripotent stem cells.

### INTRODUCTION

Direct reprogramming of human somatic cells by ectopic expression of *OCT4*, *SOX2*, *KLF4*, and *c-MYC* (OSKM) transcription factors results in generation of human-induced pluripotent stem cells (hiPSCs), which are similar to human embryonic stem cells (hESCs) in many of their properties [1]. Human iPSCs have been generated from various cell types [2–4] and have a great potential for regenerative medicine, because they enable the derivation of patient-specific pluripotent cells and serve as a platform for stem-based research, disease modeling, and

drug discovery/repurposing [5–9]. Despite extensive research toward understanding of the reprogramming process, the underlying mechanisms are not fully understood [10–12], hindering their effective application in clinical studies [13]. A number of molecular and cellular barriers of reprogramming have been identified to date [14–16], resulting in an overall 2%–5% efficiency, thus indicating that the majority of cells are unable to complete reprogramming toward pluripotency [17–19].

Pluripotency induction during reprogramming occurs in discrete stages (initiation, maturation, and stabilization) and is characterized by specific

alterations in the cellular transcriptome, epigenome [20–22], and stage-specific modulation of various signaling pathways some of which have been recently elucidated in our recent publications [17, 18]. Chemical inhibition of glycogen synthase kinase 3 [23], transforming growth factor  $\beta$  (TGF- $\beta$ ) signaling [23, 24], and inhibition of mitogen-activated protein kinase (MAPK) signaling promote early stages of reprogramming, whereas the inactivation of Rb tumor suppressor promotes reprogramming and increases its efficiency [25]. Activation of phosphoinositide3-kinase (PI3K)-AKT signaling, and focal adhesion (FA) as well as regulation of actin cytoskeleton, is required during the transition of fibroblasts to the pluripotent state [26].

To identify novel regulators of reprogramming, we developed a high-throughput RNA interference (RNAi) screening assay. This strategy allowed us to perform knockdown of 784 members of the different kinases and phosphatases at the initiation stage of reprogramming. We identified 90 reprogramming candidates: 68 repressors and 22 activators, among which 76 were novel. Importantly, our list included previously recognized candidates in human (MPP3, TGFBR1, BUB1B, BMPR2, AKT1, NME5, ROCK2, RPS6KB2, TESK1, BMPR2, MELK, and SPHK2) and mouse cells (Act1, Acvr11, Tgfr1, and Rps6kb2) [11, 15, 27–29]. Among the top effectors, three members of the G protein-coupled receptors (GPCRs) family, namely GPR42, GPR20, and endothelial differentiation GPCR5 (EDG5) were identified. In addition, three other GPCRs, GPR123, GPR116, and GPR37L1 were identified in our screen as potential reprogramming effectors.

There are more than 800 GPCRs in the human genome, making it the largest receptor superfamily of cell-surface signaling proteins that bind extracellular ligands and transduce signals into cells via heterotrimeric GTP-binding (G) proteins. The human GPCR superfamily is divided in five distinct families: rhodopsin, secretin, glutamate, adhesion, and frizzled receptors. G-proteins, composed of  $\alpha$ ,  $\beta$ , and  $\gamma$  subunits, are central components of the primary mechanisms used by cells to respond to diverse extracellular stimuli. Most GPCRs activate one or multiple G-alpha ( $G\alpha$ ) subunits, which can be subdivided into four major families: Gi, G12/13, Gs, and Gq. Once activated, G protein subunits modulate secondary messenger release and activate various downstream intracellular signaling pathways (including adenylyl cyclase, phospholipases A2, C (PLC), and D, calcium mobilization, MAPK, extracellular signal-regulated kinases-1/2 ERK[1/2], PI3K, and the activation of small GTPases such as Rho and Rac), leading to regulation and adaptation of cellular functions to an external stimulus.

Knockdown of some GPCRs and/or components of their signaling pathways (Gs subunit, for example) are embryonic lethal or associated with significant developmental anomalies in mice and humans [30]. However, despite the fundamental role of GPCRs and G proteins, their function during development and reprogramming process remains largely unexplored. A recently published report indicates that 116 GPCRs are expressed in hESCs, with 39 of these being upregulated and 20 downregulated during somatic reprogramming to hiPSC. Furthermore, 106 GPCRs are upregulated in hESC and hiPSC when compared to somatic cells, suggesting a putative role in maintenance of pluripotency or early differentiation [31, 32]. This is further supported by the published reports, showing

the Gs pathway and cAMP to be important contributors of mouse and human ESC self-renewal and pluripotency [33, 34].

Two known positive regulators of pluripotency in hESCs, sphingosine-1-phosphate (S1P), and lysophosphatidic acid [35, 36], act via a single subfamily of GPCRs, designated as endothelial differentiation gene (EDG) family. The five EDG receptors specific for S1P are coupled to overlapping yet distinct sets of intracellular signaling pathways. Recently *EDG5* was identified as a novel gene required for stem cell pluripotency [37]. However, until now, there are no detailed studies dedicated to the role of this gene during reprogramming of somatic cells toward hiPSCs. We investigated the function of *EDG5* in maintenance of pluripotency in hESC and during somatic cell-induced reprogramming of human neonatal fibroblasts (HNFs). Our data indicate that *EDG5* is important for the maintenance of colony morphology, organization of actin cytoskeleton and FAs, and the suppression of mesoendodermal gene expression in hESC. Similarly, downregulation of *EDG5* during the initiation stage of reprogramming process resulted in loss of colony integrity, dysregulation of actin cytoskeleton, and a significant reduction in the number of pluripotent stem cell colonies. Together, our data provide for the first time, substantive evidence for *EDG5* as a critical GPCR for the maintenance of pluripotency in hESC and successful reprogramming of human fibroblasts to hiPSCs.

## MATERIALS AND METHODS

### hiPSCs Generation and Cell Culture

CytoTune-iPS 2.0 Sendai reprogramming kit (A16517, Invitrogen, Fisher Scientific UK Ltd; Loughborough, UK) was used for iPSC derivation as described recently on a feeder-free culture on a plates covered with Matrigel (Corning Matrigel Matrix, Life Sciences, hESC-qualified, High Wycombe, UK) [17]. HNFs were purchased from Lonza (Slough, UK) and were cultured as described earlier [17].

### RNA Interference

SMARTpool: siGENOME small interfering RNA (siRNA) for *EDG5* was purchased from Dharmacon (M-004253-02-0005; Supporting Information Table S1). The siRNA mixture at final concentration of 10 nM was used for transfection with DharmaFECT1 Transfection reagent (Dharmacon, Cambridge, UK, T-2001-01) according to manufacturer's instructions with OPTI-MEM reduced serum Media (31985-062; Gibco, Dublin, Ireland) for the first 45 minutes of transfection. Then an equal volume of the mTeSR1Medium (STEMCELL Technologies, Cambridge, UK) was added to cells. Media was changed for mTeSR1 every day. As a control ON-TARGETplus nontargeting control pool from Dharmacon (D-001810-10) was used.

### Western Immunoblotting

Protein extraction, Western blotting, and antibody/antigen complex detection were performed as published previously [17]. NEPER nuclear and cytoplasmic extraction reagent (78835) from ThermoScientific was used for nuclear and cytoplasmic extraction according to manufacturer protocol. Densitometry analysis was performed using ImageQuant TL software (GE Healthcare Life Sciences). Glyceraldehyde-3-phosphate dehydrogenase (GAPDH) was used to normalize band intensities of proteins of interest.

Primary antibodies were from Cell Signaling: for phospho-cofilin (Ser3) (77G2, 3313), for total Cofilin (D3F9; 5175), for GAPDH (14C10; 2118), for Phospho-FAK (Tyr397; D20B1; 8556), for total FAK (3285), for p-MLC2 (Ser19; 3671), for TESK1 (D4904), for NANOG (D73G4; 4903), and for p-ERK Thr202/Tyr204 (D13.14.4E). Primary antibodies from Abcam (Cambridge, UK) were: for PAXILLIN (phospho Y118; ab194738), for total PAXILLIN (ab2264), for ROCK1 (ab58305), and for GAPDH (ab9485). Antibody for p-LIMK2 (Thr505) was from Invitrogen (PA537630). Primary antibodies from Santa Cruz (Heidelberg, Germany) were: for EDG5 (E-12; sc365963), for vinculin (H-10; sc-253360), and for GAPDH (sc-47724). Antibody for E-cadherin was from ThermoFisher Scientific (5H6L18; 701134).

### Immunocytochemistry and Confocal Microscopy

Immunocytochemistry was performed as before [18]. Primary antibodies used in this study were anti-TRA-1-60 FITC conjugate (Merck Millipore, Watford, UK), anti-EDG5 (E-12) sc-365963, anti-NANOG cell signaling 4903, anti-p-Cofilin (Ser3; 77G2; 3313) cell signaling, anti-p-FAK (Tyr397; D20B1; 8556) cell signaling, anti-p-PAXILLIN (Tyr1218) ab194738, anti-E-cadherin (Cell Signaling Technology, New England BioLabs Ltd., Hitchin, UK), and 4',6-diamidino-2-phenylindole was from ThermoFisher. Rhodamine phalloidin from Life Technologies (R415) was used for visualization of filamentous actin. The images were acquired with a Nikon A1R laser scanning confocal microscope (Nikon; <http://nikon.com>) using a CFI Plan Aplanochromat VC  $\times 20/0.75$  objective as described [18].

### Quantitative Reverse Transcription Polymerase Chain Reaction

Cells were harvested, and the total RNA was extracted using TRIzol (Invitrogen, 15596-026), according to manufacturer's instructions. All steps were performed as described before [18]. Samples were normalized using GAPDH. All DNA oligonucleotide sequences are listed in Supporting Information Table S1.

### Flow Cytometric Analysis

Cells were disassociated using Versene (EDTA; Lonza), washed with phosphate-buffered saline (PBS), and fixed in paraformaldehyde (2% final concentration in PBS) at 37°C for 10 minutes. After washing with PBS, the cells were permeabilized with pre-chilled methanol (−20°C) and incubated at 4°C for 30 minutes, followed by a washing step. Cells ( $0.2\text{--}0.5 \times 10^6$ ) were resuspended in a total volume of 200  $\mu\text{l}$  PBS containing 1% bovine serum albumin and incubated with appropriate amounts of anti-CD44-BV421 (Catalog number 562890; BD Biosciences, Oxford, UK; 1:300 dilution) and anti-TRA-1-60-FITC (Catalog number FCMAB115F; Merck Millipore; 1:100 dilution) monoclonal antibodies for 1 hour on a shaker, plate in the dark at room temperature. Finally, samples were washed using BD FACS Lyse Wash Assistant (BD Biosciences) and immediately analyzed on a flow cytometer. Fluorescence-activated cell sorting (FACS) analysis was performed using BD FACS Canto II flow cytometer with FACSDiva software (BD Biosciences). A minimum of 20,000 events were recorded for each sample. Fluorescence minus one control (for each antibody) was used to gate the subpopulations.

Alkaline phosphatase detection was performed with alkaline phosphatase detection kit (SCR004; Millipore) according to manufacture instructions.

### Statistical Analysis

Student *t*-test analysis was used to assess differences between control and EDG5-RNAi groups. The results were considered significant if  $p < .05$ . Significant differences indicated using asterisks (\*,  $p < .05$ ; \*\*,  $p < .01$ ).

## RESULTS

### Identification of New Genes Important for Reprogramming of Human Fibroblasts

To identify new candidate genes involved in hiPSCs generation, we developed a high-throughput assay adapted to a 384-well format for genome-wide siRNA screening using the Dharmacon library (Fig. 1A). We performed siRNA-mediated knockdown of 784 members of the different kinases and phosphatases family members within a specific phase: days 8–10 of reprogramming. We choose this period of reprogramming because at this time many cellular events (such mesenchymal to epithelial transition, increased cell proliferation, changes in cellular metabolism, and cytoskeleton remodeling) which are important for hiPSC generation take place [17, 18]. Cells were examined via automated cell imaging for the expression of the cell surface pluripotency marker TRA-1-60 at day10 (Fig. 1A). The average Z scores from three biological repeats were calculated for TRA-1-60+ cells versus total nuclei and a cutoff of  $\pm 1.65$  was applied. This analysis resulted in identification of 68 candidate repressors and 22 candidate effectors, which included genes reported to play an important role in hiPSC generation, including *MPP3*, *TGFBR2*, *ROCK1*, *ATM*, *BUB1*, and *TESK1* (Supporting Information Fig. S1A) [11, 15, 27–29]. Gene ontology-enrichment pathway analysis of these candidate repressors and effectors showed enrichment of multiple biological processes and pathways, which included known (e.g., AKT, ERK, and apoptosis) and novel regulators (GPCRs) of reprogramming (Fig. 1B, 1C). Importantly, we identified six genes belonging to the GPCR family, namely *EDG5*, *GPR42*, *GPR20*, *GPR123*, *GPR116*, and *GPR37L1* as candidate effectors of the reprogramming process (Fig. 1B; Supporting Information Fig. S1A).

Our examination of the expression of the named GPCR candidates in hESC and hiPSC compared to somatic cells using publicly available microarray expression data [32] indicated that out of the six genes of interest, three, namely *EDG5*, *GPR20*, and *GPR123* were significantly upregulated in hESCs and hiPSCs versus somatic cells, suggesting a putative role for pluripotency acquisition and maintenance (Fig. 1D). Thus, to get new insights into their function during somatic cell-induced reprogramming, we focused our attention on *EDG5*, also known as S1P receptor 2 (*S1P2*).

### Downregulation of EDG5 Abrogates hiPSCs Generation

Immunofluorescence analysis demonstrated expression of EDG5 on the surface, cytoplasm, and nucleus of hESCs (Fig. 2A). Western blot analysis revealed higher expression of EDG5 in hESCs versus HNFs (Fig. 2B). To validate the results of high-throughput screening, we downregulated the expression of *EDG5* by RNAi at day 8 of reprogramming (Fig. 2C, 2D) and assessed the number of alkaline phosphatase positive colonies at day 28. This analysis indicated a significant reduction in the number of alkaline phosphatase of pluripotent stem cell

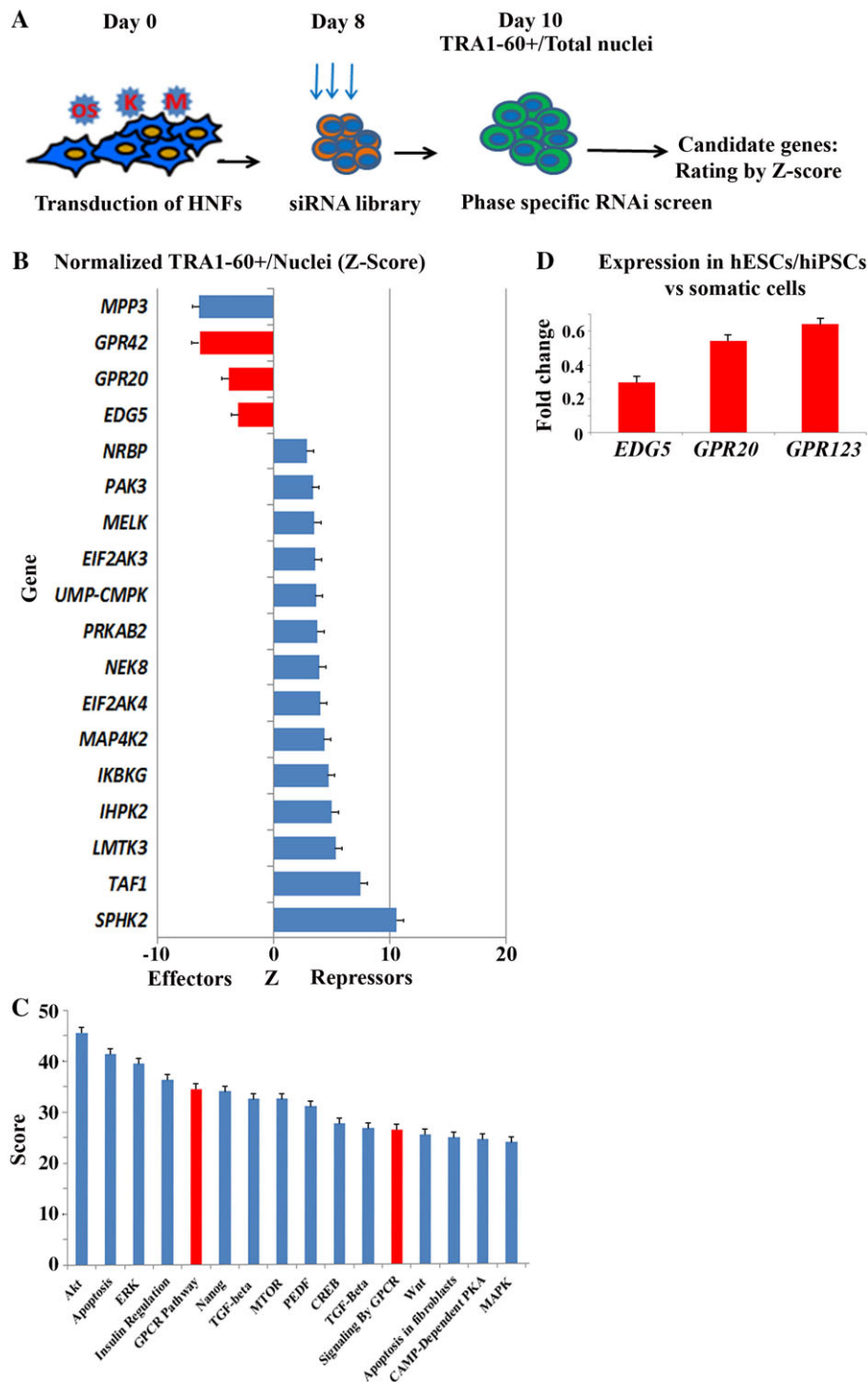


**Figure 1.** High-throughput RNAi screen for regulators of somatic cell reprogramming. **(A):** Graphical flow of the experimental design. HNFs were transduced with *OCT4*, *SOX2*, *KLF4*, and *c-MYC* (OSKM) and on the day 8 of reprogramming RNAi to 784 genes were applied to cells transferred to 384 well-plate format. Colonies were examined at day10 via automated cells imaging for the expression of pluripotency cell surface marker TRA1-60 (green) at day 10. All nuclei were stained with 4',6-diamidino-2-phenylindole. Total area for green colonies (TRA1-60+) over the total number of nuclei was used for statistical analysis: average Z-score was applied with cutoff of  $\pm 1.65$  with error at 0.005 to reveal candidate genes; **(B):** Z-score-ranked distribution plot for the RNAi screen at day 10 post OSKM transduction. Top candidates are shown here, and the full list supplied in Supporting Information Figure S1. The top three new effectors belonging to the GPCRs family *GPR42*, *GPR20*, and *EDG5* are shown in red; **(C):** Graphical representation of the gene ontology-enriched signaling pathway analysis of 90 candidate genes; **(D):** graphical representation of the overexpression of *EDG5*, *GPR20*, and *GPR123* in pluripotent cells over 100 of human somatic cells analyzed from publicly available data [32]. Abbreviations: GPCR, G protein-coupled receptor; hESC, human embryonic stem cell; hiPSC, human-induced pluripotent stem cell; HNF, Human neonatal fibroblast; MAPK, mitogen-activated protein kinase; PEDF, Pigment Epithelium Derived Factor; PKA, protein kinase-A; RNAi, RNA interference; siRNA, small interfering RNA; TGF, transforming growth factor.

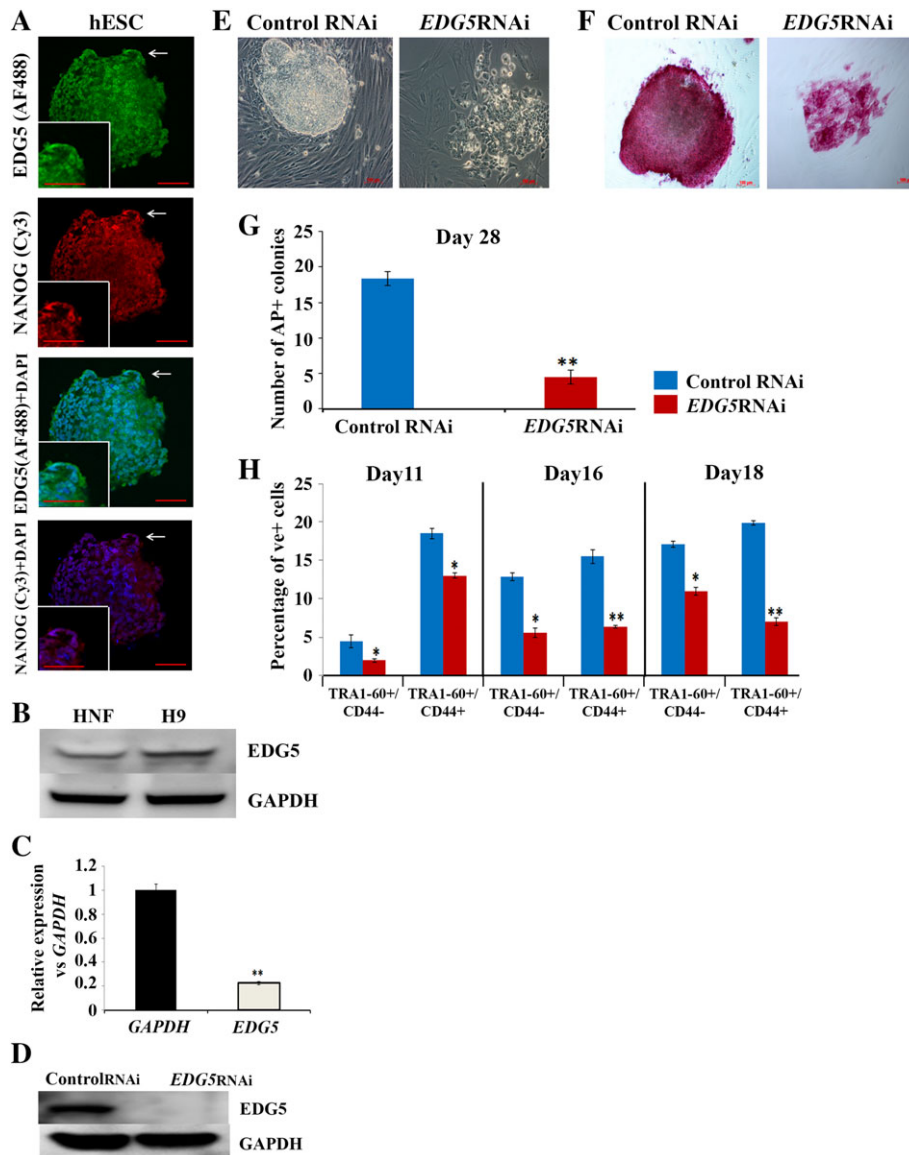


**Figure 2.** Downregulation of *EDG5* abrogates human-induced pluripotent stem cells generation. (A): Immunofluorescence observation of the *EDG5* expression in hESCs. Scale bar 100  $\mu$ m. White arrows point to the area of interest, which is shown at higher magnification in the inset. Representative examples of at least three independent experiments are shown; (B): Representative Western blot analyses of the *EDG5* expression in HNF and hESCs (H9),  $n = 3$ ; (C): Real-time quantitative polymerase chain reaction analysis of the relative expression of *EDG5* versus *GAPDH* under *EDG5*-RNAi in hESCs. Data are shown as mean  $\pm$  SEM,  $n = 3$ , with significance difference indicated with asterisks (\*\*,  $p < .01$ ); (D): Representative Western blot analysis of *EDG5* in hESCs transfected with control and *EDG5*siRNA,  $n = 3$ . *GAPDH* serve as a loading control. (E, F): Representative images depicting typical colonies morphology at brightfield (E) and AP+ staining for control and *EDG5*siRNA-treated colonies (F) at day 28 of reprogramming. (G): Graphical representation of the number of the AP+ colonies at day 28 of reprogramming upon *EDG5* knockdown at days 8–10 of reprogramming process. Data are represented as mean  $\pm$  SEM,  $n = 3$  (\*\*,  $p < .01$ ); (H): flow cytometry analysis of different subpopulations during the time course (at day 11, day 16, and day 18) of reprogramming in control and *EDG5*siRNA-treated groups. Data are represented as mean  $\pm$  SEM,  $n = 3$ , with significant differences indicated using asterisks (\*,  $p < .05$ ; \*\*,  $p < .01$ ). Abbreviations: AP, alkaline-phosphatase; DAPI, 4',6-diamidino-2-phenylindole; hESC, human embryonic stem cell; HNF, human neonatal fibroblast; *GAPDH*, glyceraldehyde-3-phosphate dehydrogenase; RNAi, RNA interference.

colonies (Fig. 2E–2G), thus confirming the data of the high-throughput RNAi screen and suggesting that the GPCR family member, *EDG5*, may have an important role during the initiation stage of reprogramming process. To address which subpopulations were affected by *EDG5* knockdown, we performed flow cytometric analysis (Fig. 2H) which indicated a significant reduction in the percentage of fully and partially reprogrammed cells represented by the TRA1-60+/CD44- and TRA1-60+/CD44+ subpopulations, respectively, thus suggesting that the impacts of

*EDG5*RNAi at the early stages of reprogramming were irreversible.

#### Downregulation of *EDG5* Changes Colony Morphology and Induces Differentiation in hESCs

To address the role of *EDG5* in hESC, we performed RNAi (Fig. 3A). Downregulation of *EDG5* was confirmed using Western blotting (Fig. 3B). Downregulation of pERK was also observed, suggesting that similarly to other cell types (hepatoma cells,

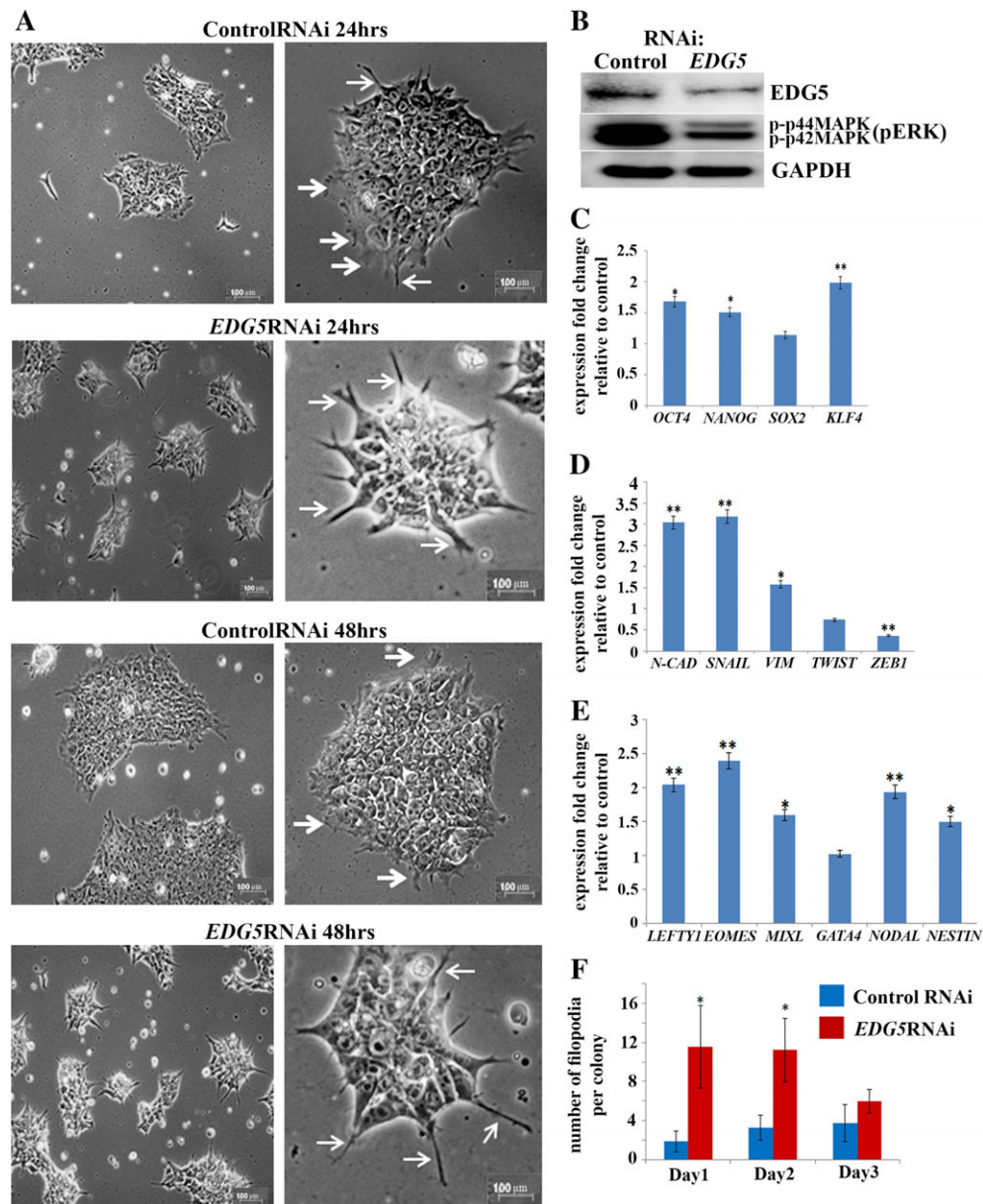


**Figure 3.** Downregulation of *EDG5* results in changes in human embryonic stem cells (hESCs) colony morphology and increased expression of differentiation marker genes. **(A):** Representative brightfield images showing hESCs colony morphology at 24 and 48 hours of transfection with control and *EDG5* small interfering RNAs (siRNAs). Thick white arrows point to lamellipodia, thin arrows-like to the filopodia-like projections. Scale bar 100  $\mu$ m,  $n = 3$ ; **(B):** Representative Western blot analysis of the *EDG5* and pERK expression in control and *EDG5*-RNAi hESCs groups. Glyceraldehyde-3-phosphate dehydrogenase serve as a loading control,  $n = 3$ ; **(C–E):** Real-time quantitative polymerase chain reaction analysis of *OCT4*, *NANOG*, *SOX2*, and *KLF4* pluripotency marker **(C)** of *E-cadherin*, *N-cadherin*, *SAIL*, *VIMENTIN*, *TWIST*, and *ZEB1* markers **(D)** and mesodermal markers *LEFTY1*, *EOMES*, *MIXL*, *GATA4*, *NODAL*, and *NESTIN* in **(E)**, data presented as mean  $\pm$  SEM,  $n = 3$  (\*,  $p < .05$ ; \*\*,  $p < .01$ ); **(F):** Graphical assessment of the number of filopodia per colony in control and *EDG5*siRNA-treated hESCs colonies at 3 days post-transfection. **(C–F):** Data presented as mean  $\pm$  SEM,  $n = 3$ ; \*,  $p < .05$ . Abbreviation: RNAi, RNA interference.

CHO-K1, and glioma cells) *EDG5* in hESCs may transduce its signal via G12/13 and Gi subunits, which signal and participate in pathway leading to activation of the MAPK protein ERK [36, 38]. Morphological assessment revealed the presence of long filopodia-like projections and larger gaps between cells within the colony (Fig. 3A). As colony integrity and morphology is one of the characteristic features of the pluripotency, we examined pluripotency and differentiation markers expression. Quantitative reverse transcription polymerase chain reaction revealed increased expression of *OCT4*, *NANOG*, and *KLF4*

(Fig. 3C), in support of the observation that some cells in *EDG5*-RNAi colonies are positive for alkaline phosphatase staining (Fig. 2F, 2G). At the same time, *EDG5* knockdown induced a significant upregulation of *N-cadherin* and *SNAIL* (Fig. 3D). Unlike *E-cadherin*, *N-cadherin* is not expressed in hESCs; instead, it is rapidly upregulated in both human and mouse ESC upon start of differentiation in a process akin to epithelial-to-mesenchymal transition (EMT) event [39]. Thus, *N-cadherin* and *SNAIL* upregulation in *EDG5* knockdown cells may mark the start of EMT transition instead of mesenchymal-to-epithelial transition (MET),

which is critical for iPSCs generation. Further analysis of the genes involved in mesodermal differentiation indicated over-expression of these markers (Fig. 3E), further supporting the start of differentiation process.

EDG5 in hESCs has been associated with the Gi, Gq, and G12/13 signaling [36], with possible preferential activation of G12/13, important for Rho small GTPase signaling [31]. Rho-ROCK signaling itself has been shown to be important for the integrity of the stem cell colony, thus supporting stem cell maintenance [40,41]. Rho family members have been implicated in regulation of the assembly of the multimolecular focal complexes associated with actin stress fibers, lamellipodia, and filopodia formation [42]. The mechanisms of lamellipodia and filopodia formation in hESCs are not well-understood but Rho family proteins, Rac, Cdc42, and RhoG have been shown to play a central role in regulation of protrusion in other cell types [43]. In addition, in G12/13-deficient mouse embryonic fibroblasts (MEFs), G13 subunit was shown to play an important role in membrane ruffles and lamellipodia formation [44]. Our analysis indicated a significant reduction in lamellipodia

and a dramatic increase of filopodia-like protrusions at 24 and 48 hours after *EDG5* knockdown (Fig. 3F), corroborating data for G12/13-deficient MEFs [44]. Together, our data suggest that *EDG5* knockdown leads to upregulation of differentiation markers and an increase in filopodia formation, which will be explored further in the following results section.

#### **EDG5 Downregulation Abrogates RhoA-ROCK Signaling and Results in Cytoskeleton Dysregulation in hESCs**

It is well-established that G12/13-coupled GPCRs signaling leads to the activation of RhoA, which plays a central role in the organization of the actin cytoskeleton through its ability to stimulate the formation of actomyosin-based structures [45], regulation of microtubule dynamics, stress fiber formation, and transcriptional activity [43]. This led us to examine the possible effects of *EDG5* downregulation on the EDG5-G12/13-RhoA-ROCK axis.

Western blot analysis indicated downregulation of RhoA and ROCK upon knockdown of *EDG5* in hESCs, whereas stimulation of EDG5 by S1P had the opposite effect on RhoA expression (Fig. 4A; Supporting Information Fig. S2A-S2A').

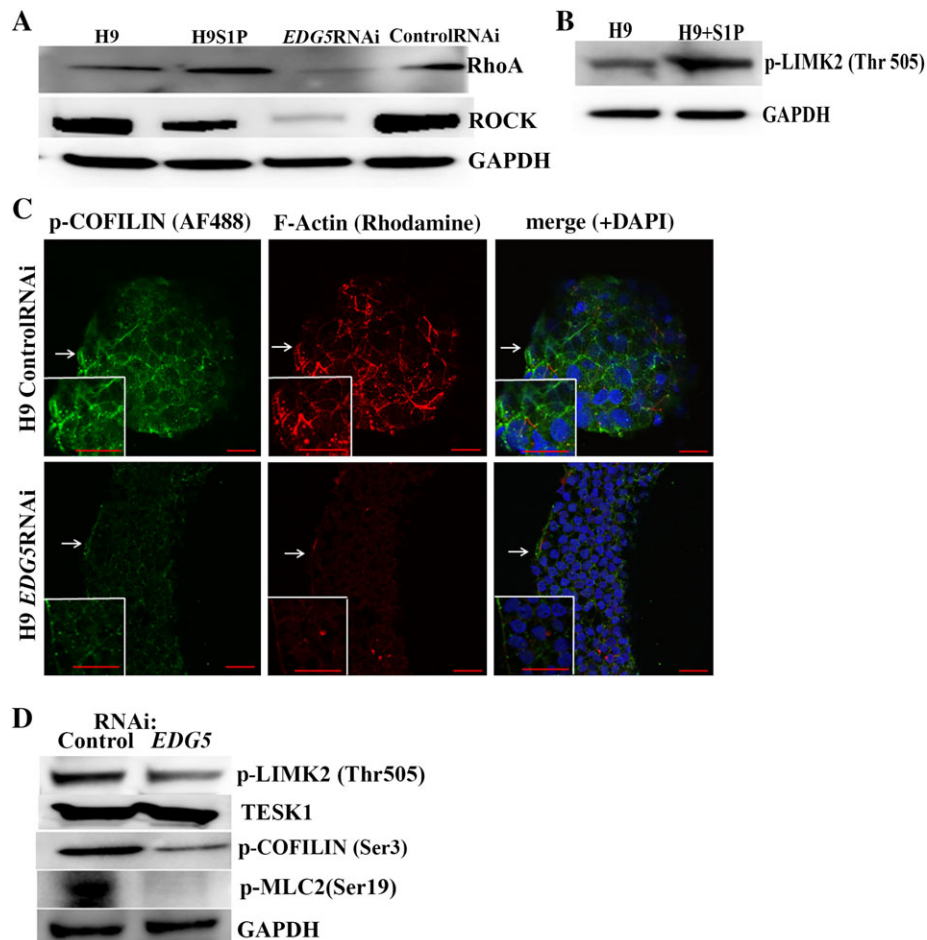


**Figure 4.** *EDG5* downregulation abrogates RhoA-ROCK signaling and induces alteration in COFILIN/F-actin cytoskeleton organization in human embryonic stem cells (hESCs). **(A):** Representative Western blot analysis of RhoA and ROCK expression in hESCs (H9), hESCs stimulated with 20  $\mu$ M S1P for 90 minutes (H9S1P), *EDG5*-RNAi hESCs, and control RNAi hESCs. GAPDH used as a loading control,  $n = 3$ ; **(B):** representative Western blot analysis of p-LIMK2 (Thr505) in hESCs (H9) and hESCs stimulated with 20  $\mu$ M S1P for 90 minutes. GAPDH-loading control,  $n = 3$ ; **(C):** representative immunofluorescence images of hESCs colonies treated with *EDG5* and controls small interfering RNAs (siRNAs) for 72 hours. White arrows point to the area of interest which is shown at higher magnification in the inset. Scale bar = 100  $\mu$ m,  $n = 3$ ; **(D):** representative Western blot of p-LIMK2 (Thr505), TESK1, p-COIFILIN (Ser3), and p-MLC2 (Ser19) expression in hESCs colonies after 72 hours from *EDG5* and controls siRNAs,  $n = 3$ . Abbreviations: GAPDH, glyceraldehyde-3-phosphate dehydrogenase; RNAi, RNA interference; S1P, sphingosine-1-phosphate.

Stimulation of EDG5 by S1P also induced an increase in p-LIMK2 (Thr505) form, suggesting an upstream role for EDG5 in COFILIN phosphorylation (Fig. 4B; Supporting Information Fig. S2B). It is known that active ROCK phosphorylates LIMK2 at Thr505 (but not LIMK1), increasing its kinase activity toward COFILIN [46]. The COFILIN/actin depolymerizing factor family of proteins plays a critical role in actin depolymerization, which is essential for recycling actin subunits to support new filament growth. As we detected reduced protein expression of RhoA and ROCK under *EDG5*-RNAi, we performed immunocytochemistry, which revealed a significant loss of prominent staining for p-COIFILIN(Ser3) and filamentous actin under *EDG5*-RNAi conditions in hESCs (Fig. 4C). These observations were supported by Western blotting analysis, which demonstrated reduction in expression of p-LIMK2 (Thr505) and p-COIFILIN (Ser3) (Fig. 4D; Supporting Information Fig. S2C). In addition to LIMK2, TESK1 is another regulator of COFILIN, as both have been shown to phosphorylate and inactivate COFILIN at Ser3, thus behaving as an actin severing factor [27]. Western blot analysis did not detect changes in TESK1 expression (Fig. 4D; Supporting Information Fig. S2C), suggesting that TESK1 is not a downstream effector of the RhoA-ROCK signaling in our experimental settings [47]. Work performed in other cell types (Chinese hamster ovary (CHO) cells and fibroblasts [48]) has shown that activation of the EDG5 results in RhoA-dependent increase in myosin light chain (MLC) phosphorylation and prominent stress fiber formation. Nonmuscle MLC2 has been described as a key substrate for ROCK signaling in hESCs [40].

Given the downregulation of Rho and ROCK upon *EDG5* knockdown, we investigated the expression of phosphorylated form of MLC2, which was also downregulated as demonstrated by Western blot analysis (Fig. 4D; Supporting Information Fig. S2C). In conclusion, these data indicate that both consecutive pathways were important for actin cytoskeleton organization, namely Rho-ROCK-LIMK2-p-COIFILIN and Rho-ROCK-p-MLC2 were compromised under *EDG5*-RNAi in hESCs.

### Downregulation of *EDG5* Disrupts PAXILLIN Cytoskeleton and FA in hESCs

Another component of the hESCs cytoskeleton shown to be important for colony morphology is PAXILLIN [49]. PAXILLIN is a multidomain protein that localizes primary to sites of cell adhesion to extracellular matrix, called FAs. hESCs and hiPSCs display large, PAXILLIN-positive FA at the edge of the colonies. A strong contractile actin fence and large adhesions have been shown to be important for maintaining hESCs colony morphology [50]. We examined the effect of the *EDG5* knockdown on PAXILLIN cytoskeleton of hESCs (Fig. 5A, 5B). Our results indicate that p-PAXILLIN (Tyr118) is lost from FAs sites upon *EDG5*-RNAi conditions (Fig. 5A, 5B; Supporting Information Fig. S3A): the same was found under ROCK inhibition (data not shown). FAK is a substrate for ROCK; in accordance, the expression of p-FAK (Tyr397) and the total FAK were significantly reduced upon *EDG5* knockdown in hESCs (Fig. 5C; Supporting Information Fig. S3B), thus suggesting that FA is

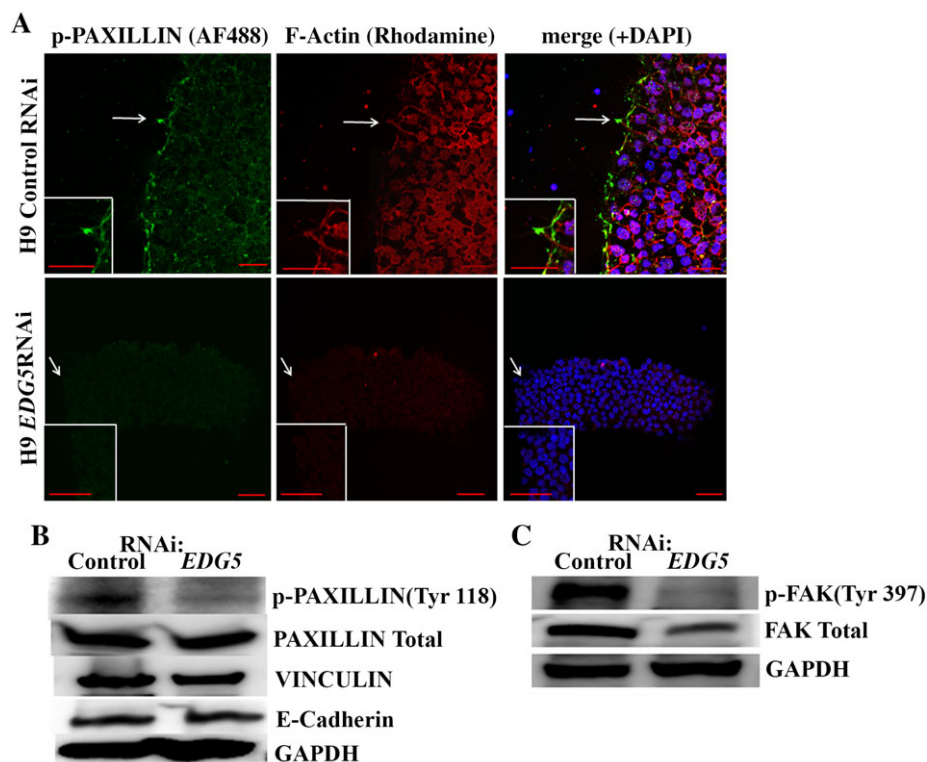


**Figure 5.** PAXILLIN cytoskeleton and focal adhesion are altered upon downregulation of *EDG5*. **(A):** Representative immunofluorescence staining for p-PAXILLIN (Tyr118) and F-actin in control and *EDG5* small interfering RNA (siRNA)-treated human embryonic stem cells (hESCs). White arrows point to the area of interest, which is shown at higher magnification in the inset.  $n = 3$ . Scale bar 100  $\mu\text{m}$ . **(B, C):** Representative Western blot analysis of p-PAXILLIN (Tyr118), PAXILLIN Total, VINCULIN, and E-cadherin in control and *EDG5*siRNA-treated hESCs. GAPDH used as a loading control,  $n = 3$ . Abbreviations: DAPI, 4',6-diamidino-2-phenylindole; GAPDH, glyceraldehyde-3-phosphate dehydrogenase; RNAi, RNA interference.



also affected in hESC (in addition to the COFILIN-PAXILLIN-F-actin cytoskeleton) as result of *EDG5* downregulation.

### Downregulation of *EDG5* Induces Alteration in the Cytoskeleton and Loss of FAs at hiPSCs During Somatic Reprogramming

In hiPSCs, FAs act as a functional signaling platform for p-FAK (Tyr 397) and p-PAXILLIN (Tyr118) and a “cornerstone” for the successful generation of hiPSCs colonies [50]. In agreement with our observation in hESCs, immunofluorescence analysis of the p-COFILIN-F-actin and p-PAXILLIN-F-actin organization at the hiPSCs colonies at day 10 post-transduction demonstrated

the presence of a ring-like structure around the hiPSC colonies, which showed the expression of p-COFILIN, p-PAXILLIN, and F-actin (Fig. 6A). Knockdown of *EDG5* from days 8 to 10 of reprogramming abolished the presence of p-COFILIN and p-PAXILLIN and disrupted the filamentous actin structures at the edge of the colonies (Fig. 6A, 6B), leading to disperse spreading of the cells within the newly emerging colonies and development of filopodia-like protrusions (black arrows, Supporting Information Fig. S5), akin to morphological features we observed in hESC upon *EDG5* downregulation (Fig. 3A). In contrast to the control colonies, colocalization of p-FAK (Tyr397) with p-PAXILLIN (Tyr118) was not observed at the

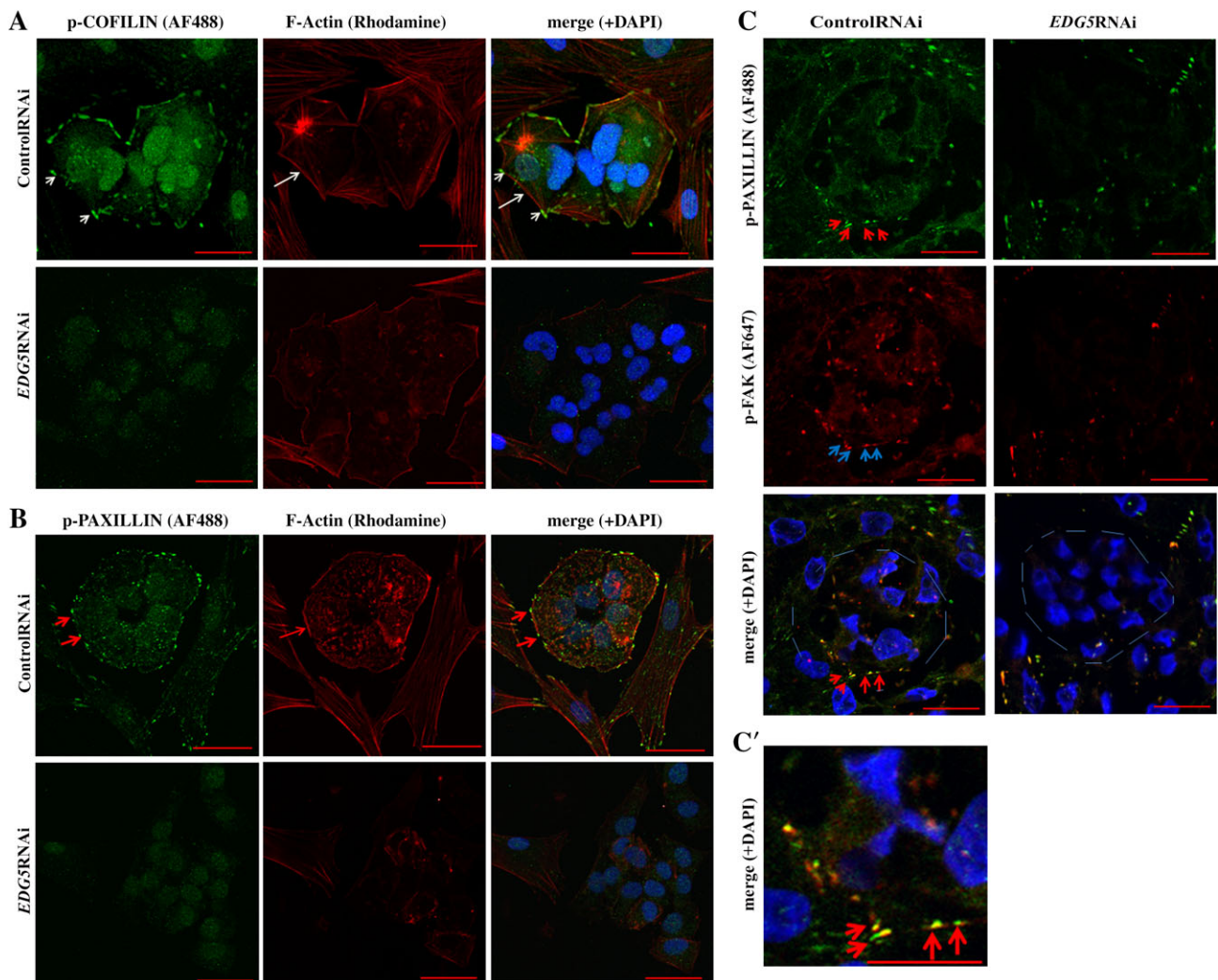


**Figure 6.** Downregulation of *EDG5* during reprogramming effect COFILIN/PAXILLIN/F-actin organization in newly formed colonies. **(A–C):** Typical confocal fluorescence images showing p-COFILIN (Ser3), p-PAXILLIN (Tyr118), p-FAK (Tyr397), and F-actin stained as indicated in colonies emerging at day 10 of *OCT4*, *SOX2*, *KLF4*, and *c-MYC* transduction and treated with control or *EDG5* small interfering RNA (siRNA) from day 8 to day10 of reprogramming,  $n = 3$ . **(A):** Short white arrows point to localization of p-COFILIN (Ser3). Long white arrow pointed to F-actin thick fibers. Note that a thick bundle of F-actin surrounds the colony. **(B):** Short red arrows point to p-PAXILLIN; long red arrow points to the F-actin. Note at the merge images, colocalization of p-COFILIN **(A)** and p-PAXILLIN **(B)** with F-actin at the end of F-actin fibers. None of such structures can be observed in *EDG5*siRNA-treated groups. Representative images from at least three independent biological replicates are shown. **(C–C’):** Red arrows pointed to p-PAXILLIN (Tyr118) with the focus plane for focal adhesions sites at control colonies; blue arrows pointed for p-FAK (Tyr397) at the sites of focal adhesions and at the merged images; red arrows pointed for colocalization of p-PAXILLIN and p-FAK at the control colonies, while no such pattern of expression can be seen at *EDG5*-RNAi colonies. Please note that in *EDG5*-RNAi samples, some cells express p-PAXILLIN and p-FAK, but without expression or colocalization at the edges of the colonies, circled by the thin light blue lines. **(C’):** Magnification of  $\times 4$  of the merge images showing (red arrows) colocalization of p-PAXILLIN (green) and p-FAK (red) in control colonies. Abbreviations: AP, alkaline-phosphatase; DAPI, 4',6-diamidino-2-phenylindole; RNAi, RNA interference.

edges of the *EDG5*-RNAi colonies at day 10 of reprogramming (Fig. 6C, 6C'), corroborating previous data from [50] and indicating an important role for *EDG5* signaling in hiPSCs development. Surprisingly, we did not find a difference in the expression of another important component of FAs: VINCULIN. Immunofluorescence analysis of VINCULIN distribution during reprogramming did not reveal differences between the control and *EDG5* inhibited groups (Supporting Information Fig. S4), corroborating out data on hESCs (Fig. 5B; Supporting Information Fig. S3A). This may be explained by the fact that localization of VINCULIN is regulated by TESK1 via integrin signaling cascade [47]; however, TESK1 signaling is unaffected by downregulation of *EDG5* as shown in Figure 4D and Supporting Information Figure S2C. Also, in agreement with data on hESCs about unchanged expression of E-cadherin (Fig. 5B; Supporting Information Fig. S3A) in response to *EDG5* knockdown, we did not detect alteration on E-cadherin expression by immunofluorescence during reprogramming under *EDG5*-RNAi conditions (Supporting Information Fig. S4). In summary, our data suggest that downregulation of *EDG5* during the initiation stage of reprogramming results in ablation of FAs at the edges of the colonies mediated by the significant reduction of p-PAXILLIN/F-actin and FAK.

### The Role of FAK Signaling During Somatic Cell-Induced Reprogramming

Given the downregulation of p-FAK (Tyr397) and loss of colony integrity upon *EDG5*-RNAi (Fig. 5C, 6C), we went on to investigate the impact of FAK inhibition using a specific inhibitor (2  $\mu$ M, PF562271; FAKi) from day 8 till day 10 of reprogramming (to correspond with the same window when RNAi screen was performed; Fig. 1A). Morphological examination of the colonies developed under FAKi conditions and *EDG5* knockdown revealed several similarities, namely the development of protrusions, sparse distribution of the cells, and loss of clear colony edges (Fig. 7A; Supporting Information Fig. S5), further supporting our data of the importance of *EDG5*-FAK regulation for hESCs/hiPSCs. Comparison of the number of emerging intermediate colonies at day 10 demonstrated a significant reduction in the FAK-inhibited group (Fig. 7B). Flow cytometric analysis revealed that the percentage of the partially and fully reprogrammed subpopulations was significantly reduced upon FAK inhibition (Fig. 7C), suggesting a link between *EDG5* signaling and FAK and corroborating previous data about the important role for FAK in reprogramming process [50].

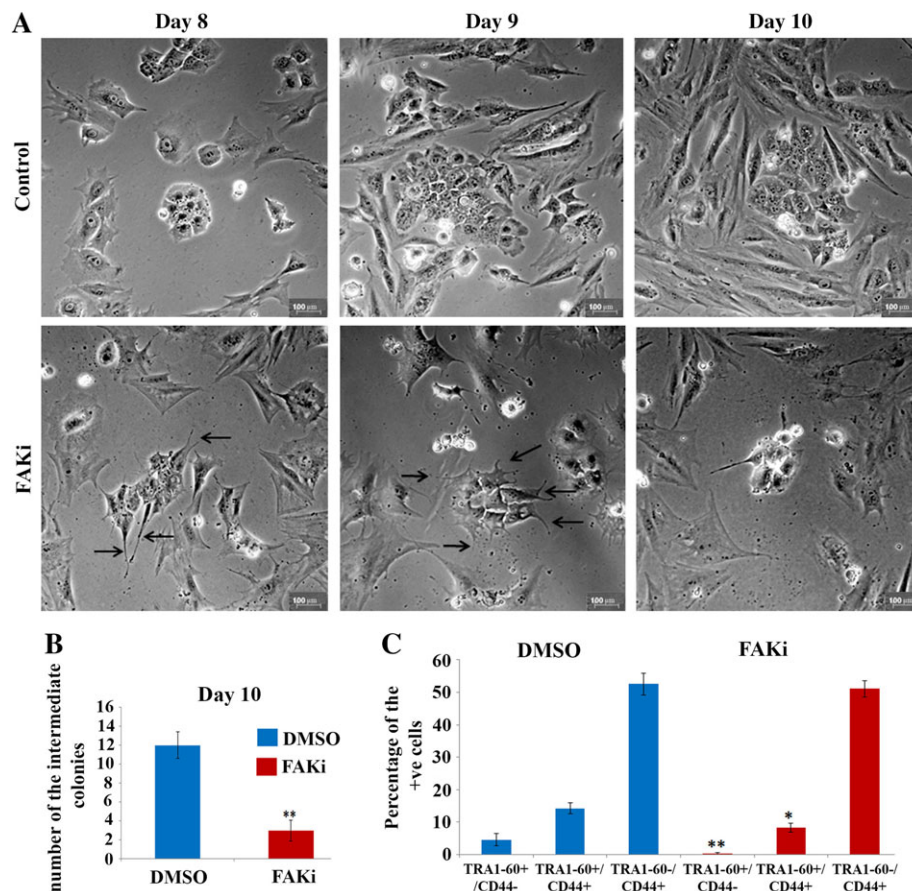


**Figure 7.** FAK inhibition abrogates colonies development during the reprogramming process. **(A):** Brightfield representative images of the typical colonies morphology developed in control (DMSO) and FAK inhibitor (2  $\mu$ M, PF562271; FAKi) groups during the time course of FAKi treatment, from day 8 till day 10,  $n = 3$ ; **(B):** graphical representation of the number of the intermediate colonies at day 10 in control Dimethyl sulfoxide (DMSO) and FAK inhibitor group (FAKi). Data are mean  $\pm$  SEM; \*\*,  $p \leq .001$ ;  $n = 3$ . **(C):** Flow cytometric analysis of TRA1-60+/CD44-, TRA1-60+/CD44+, and TRA1-60-/CD44+ subpopulations at day 10. FAK inhibitor treatment started at day 8. Data are mean  $\pm$ ;  $n = 3$ . \*,  $p < .05$ ; \*\*,  $p < .01$ .

## DISCUSSION

Since the discovery that somatic cells could be reprogrammed to iPSCs in 2006 by Yamanaka and colleagues [51], vast amount of research has been performed to try to improve the reprogramming efficiency and to better understand the molecular machinery of pluripotency acquisition and maintenance. Undoubtedly, numerous studies which reported identification of new effectors or barriers of reprogramming process have broadened our knowledge about complex interaction of the different signaling pathway and reprogramming mechanisms [11, 19, 52] and have highlighted an important role for MET, metabolism, apoptosis, cytoskeleton rearrangement, autophagy, immune response, cell cycle alterations, epigenetics, and many others for the effective hiPSCs generation.

In our research, we used a 384-well plate format for small interfering RNA (RNAi) screening of the library of 784 different kinases and phosphatases. This screening strategy allowed us to identify in addition to the known players in reprogramming new candidate effectors and repressors of this process. This screen revealed enrichment in GPCRs signaling and identified six new effectors (GPR42, GPR20, EDG5, GPR123, GPR116, and GPR37L1) belonging to this family. We focused our attention on EDG5 and showed that downregulation of *EDG5* resulted in loss of typical colony morphology, acquisition of filopodia, dysregulation of actin cytoskeleton, overexpression of mesodermal and EMT markers, and a significant reduction in the number of alkaline-positive colonies in hESCs. Similarly, downregulation of *EDG5* during the initiation stages of human somatic cell-induced reprogramming led to similar dysregulation of cytoskeleton, colony integrity, FAs, and reduced number of the pluripotent stem cell colonies at the end of the reprogramming process. Accordingly, these data imply that in hESCs, *EDG5* functions cannot be substituted by its close EDG family member, EDG3, which has been suggested to compensate for Edg5 null mice, which are viable, fertile, and developed normally [53]. Corroborating our data, it has been reported that MEFs null for EDG5 show a significant reduction in Rho activation but no effect on PLC activation, calcium mobilization, or adenylyl cyclase inhibition, suggesting preferential signaling via EDG5 to G12/13  $\alpha$  subunit, important for Rho-ROCK signaling [53]. At the same time, infection of MEFs with constitutively active G12 together with reprogramming factors led to a significant reduction in alkaline phosphatase colonies [15], suggesting that affecting the same signaling axis via one effector on the same signaling network may lead to opposite effects in different experimental condition and pointing to the complexity of the reprogramming process as well as differences in human versus mouse cells.

In hESCs, S1P receptors are linked to different G proteins, allowing this signaling pathway to elicit a variety of specific responses through the activation of Gi, Gq, G12/13, and Gs which control survival, proliferation, migration, and self-renewal [31, 35]. Our experiments suggest that EDG1 and EDG3 cannot compensate for the ablation of EDG5 signaling. The function of EDG1 and EDG3 in hESCs is not well-known; thus, additional studies are needed to understand the S1P-mediated effects on reprogramming and whether culture media supplementation with S1P rescues EDG5 downregulation. In addition, it will be of interest to investigate whether supplementation of the culture media with S1P (which in

hESCs can signal via EDG1, EDG3, and EDG5 receptors) can be beneficial for reprogramming.

Regardless the fact that G protein signaling is recognized as a key functional regulator of hiPSCs generation [11], this is the first study dedicated to the functional role of the EDG family GPCRs member, *EDG5*, in this process. As EDG5 signaling can be mediated via three different G- $\alpha$  subunits resulting in the different cellular outcomes, we focused our study to the EDG5-G12/13-RoA-ROCK signaling pathway. Our study demonstrated that *EDG5* downregulation in hESCs abrogated Rho-ROCK signaling and led to COFILIN/PAXILLIN/F-actin cytoskeleton abnormalities. Earlier, the importance of actin filament organization for human somatic cell reprogramming was suggested by [11, 28, 31] and recognized as a significant hit through identification of candidate genes involved in cell motility and adhesion during hiPSCs generation [16]. Importantly, it was shown that during MET, the actin cytoskeleton is reorganized from actin stress fibers to cortical actin, a process tightly regulated by phosphorylation of COFILIN on Ser3 by LIMK2 and TESK1 activity [27]. In agreement with this, our data demonstrated a reduction at the active form of LIMK2 and p-COFILIN (Ser3), which led to the ablation of the filamentous actin organization upon downregulation of *EDG5*. This also occurred during the somatic cell-induced reprogramming, thus highlighting for the first time that the importance of the EDG5-G12/13 signaling is the maintenance and induction of pluripotency.

It is known that actin filaments generate forces that drive changes in cell shape and mechanics through their interaction with myosin molecular motors. In fact, RhoA-GTPase/Rho-associated ROCK-myosin-II signaling can alter tension of the actin cytoskeleton and regulate survival of individual hESCs [54]. Furthermore, actin-myosin colocalization was shown to be enhanced at the edge of the colonies, and the block of myosin II activity leads to loss of colonies [55]. Our analysis for the active form of myosin II, p-MLC2 (Ser19), revealed its significant downregulation, suggesting that RhoA-ROCK-dependent pathway important for actin cytoskeleton organization and operating via phosphorylation of cofilin and MLC2 was severely dysregulated upon EDG5 knockdown, thus providing a potential mechanism for loss of hiPSC colonies during the reprogramming process. In previous reports, it has been reported that ROCK inhibition with Y-27632 for 24 hours facilitates generation of hiPSCs [56]. At first glance, these data may seem contradictory to our findings. However, it is well known that ROCK inhibition render hESCs less sensitive to the environmental changes (e.g., dissociation and detachment during single-cell propagation), thus improving their plating efficiency [57, 58]. We found that in contrast to the complete absence of the filamentous actin upon *EDG5* knockdown, inhibition of ROCK signaling pathway led to reduced staining for filamentous actin in hESCs but not complete ablation (data not shown), suggesting that a direct comparison is not valid.

The assembly of filamentous actin was shown to play a direct role in controlling cytoskeletal and morphological aspects of the contact guidance response in hESCs [59]. Thus, it can be hypothesized that remodeling of the actin cytoskeleton during the transition from the somatic to pluripotent stem cells ultimately will have an impact on the reorganization of the all cellular systems responsible for numerous biological processes as cellular movement, adhesion, substrate interaction, gene expression, and many others. Actin cytoskeleton is

widely involved in cellular movement and chemotaxis, but very little is known about regulation of these cellular functions as in hESCs/hiPSCs [60,61] and during human somatic cell reprogramming. Also, regardless of the fact that genes involved in the actin cytoskeleton remodeling were named as hits for hiPSCs generation, our understanding of the biology and regulation of these processes during reprogramming is very naive and calls for additional studies. With regards to this, it was shown that *EDG5* expressing CHO cells exhibited inhibition of migration and chemotaxis toward Insulin-like growth factor 1(IGF1) in response to the S1P concentration gradient [48], thus indicating that S1P and *EDG5*'s potential action in hESCs migration and chemotaxis are additional subjects for further study, as this may be important for single-cell clonal expansion and propagation of hiPSCs.

Another aspect of our research is the link between actin cytoskeleton and FAs during reprogramming. FAs, the cell's mechano-transducing units, were recently reported to be important for the generation of hiPSCs [50]. PAXILLIN is a multifunctional and multidomain FA adapter protein, which serves an important scaffolding role at FAs by recruiting structural and signaling molecules involved in cell movement and migration. Tyrosine 118 phosphorylation of PAXILLIN, the main residue for PAXILLIN phosphorylation by FAK, provides a scaffold for establishment of FA. Our data demonstrated that knockdown of *EDG5* resulted in loss of PAXILLIN (Thr 118) which may be important for FA-dependent regulation of cell morphology and hiPSCs development [50]. The phosphorylation of PAXILLIN by FAK has been suggested to mediate transduction from cell adhesion to the reorganization of the cytoskeleton required for cell movement [62]. Application of a specific FAK inhibitor (PF562271) during the reprogramming window resulted in a significant reduction in the number of pluripotent stem cell colonies, further supporting our data obtained with *EDG5* knockdown. Furthermore, our data provide evidence that *EDG5* plays an important role for the assembly of FAs as its downregulation resulted in significant decrease on the expression of two key components, namely p-FAK and p-PAXILLIN, in hESC and during reprogramming of human fibroblasts to hiPSC.

## SUMMARY

Using an RNAi screen at the initiation stage of reprogramming, we identified 90 new potential effectors and repressors of reprogramming. Of the 22 effectors, six new genes belonging to the GPCR family were identified. Detailed analysis of the *EDG5* (*S1P2*) downregulation in hESC and during reprogramming to hiPSC demonstrated alteration of the typical stem cell morphology, acquisition of filopodia, which was associated

with downregulation of RhoA-ROCK signaling, reduced expression of p-LIMK2 (Thr505), ablation of the p-COFLIN (Ser3) expression, and a significant reduction in filamentous F-actin. Also, our data revealed alteration at the Rho-ROCK-p-MLC2 signaling, the second axis important for actin cytoskeleton organization. Additionally, in agreement with that FAK is a substrate of ROCK, the expression of p-FAK (Tyr 397) was reduced; consequently, p-PAXILLIN (Tyr118), important for FAs organization at the edges of the colonies, was lost. Thus, we concluded that *EDG5* signaling via G12/13-RoA-ROCK is important for (a) proper F-actin cytoskeleton organization in hESCs and its remodeling during generation of hiPSCs and (b) the assembly of the PAXILLIN/F-actin-FAK FA complexes, which are important for pluripotency and colony integrity as summarized in the Graphical Abstract (Supporting Information Fig. S6). Application of the specific FAK inhibitor (PF562271) at day 8 to day 10 of the reprogramming process significantly reduced the number of developing colonies, further supporting our data. Thus, *EDG5* is a new indispensable gene for acquisition and maintenance of pluripotency.

## ACKNOWLEDGMENTS

This work was supported by the European Research Council fellowship to M.L. (614620), Innovative Medicine Initiative-STEMBANCC grant to L.A., and the Biotechnology and Biological Sciences Research Council grant BB/M00015X/2 to G.L. The authors are grateful to Newcastle University for financial support, flow cytometric facility, Dr. Alex Laude, and Lisa Hodgson for technical support.

## AUTHOR CONTRIBUTIONS

I.N.: conception/design, collection and/or assembly of data, data analysis and interpretation, figure preparation, manuscript writing, final approval of manuscript; L.C., P.B., and K.G.: collection and/or assembly of data, data analysis and interpretation, final approval of manuscript; L.A. and G.L.: conception/design, financial support, final approval of manuscript; M.L.: conception/design, data analysis and interpretation, manuscript writing, financial support, final approval of manuscript; A.S.: statistical analysis and data interpretation.

## DISCLOSURE OF POTENTIAL CONFLICTS OF INTEREST

L.C. declared employment/leadership position with Fujifilm Diosynth Biotechnologies UK Ltd. The other authors indicated no potential conflicts of interest.

## REFERENCES

- Okita K, Ichisaka T, Yamanaka S. Generation of germline-competent induced pluripotent stem cells. *Nature* 2007;448:313–317.
- Wernig M, Lengner CJ, Hanna J et al. A drug-inducible transgenic system for direct reprogramming of multiple somatic cell types. *Nat Biotechnol* 2008;26:916–924.
- Maherali N, Ahfeldt T, Rigamonti A et al. A high-efficiency system for the generation and study of human induced pluripotent stem cells. *Cell Stem Cell* 2008;3:340–345.
- Hanna J, Markoulaki S, Schorderet P et al. Direct reprogramming of terminally differentiated mature B lymphocytes to pluripotency. *Cell* 2008;133:250–264.
- Takahashi K, Tanabe K, Ohnuki M et al. Induction of pluripotent stem cells from adult human fibroblasts by defined factors. *Cell* 2007;131:861–872.
- Yu J, Vodyanik MA, Smuga-Otto K et al. Induced pluripotent stem cell lines derived

from human somatic cells. *Science* 2007;318:1917–1920.

7 Park IH, Zhao R, West JA et al. Reprogramming of human somatic cells to pluripotency with defined factors. *Nature* 2008;451:141–146.

8 Nenasheva VV, Novosadova EV, Makarova IV et al. The transcriptional changes of trim genes associated with Parkinson's disease on a model of human induced pluripotent stem cells. *Mol Neurobiol* 2017;54:7204–7211.

9 Wu SM, Hochedlinger K. Harnessing the potential of induced pluripotent stem cells for regenerative medicine. *Nat Cell Biol* 2011;13:497–505.

10 Yu Y, Liang D, Tian Q et al. Stimulation of somatic cell reprogramming by ERas-Akt-FoxO1 signaling axis. *STEM CELLS* 2014;32:349–363.

11 Toh CX, Chan JW, Chong ZS et al. RNAi reveals phase-specific global regulators of human somatic cell reprogramming. *Cell Rep* 2016;15:2597–2607.

12 Gao P, Sun C, Liao W et al. Integrative research of induction of pluripotent stem cells. *Integrative Med Int* 2017;4:115–124.

13 Cherry AB, Daley GQ. Reprogrammed cells for disease modeling and regenerative medicine. *Annu Rev Med* 2013;64:277–290.

14 Feng B, Ng JH, Heng JC et al. Molecules that promote or enhance reprogramming of somatic cells to induced pluripotent stem cells. *Cell Stem Cell* 2009;4:301–312.

15 Fritz AL, Mao SR, West MG et al. A medium-throughput analysis of signaling pathways involved in early stages of stem cell reprogramming. *Biotechnol Bioeng* 2015;112:209–219.

16 Qin H, Diaz A, Blouin L et al. Systematic identification of barriers to human iPSC generation. *Cell* 2014;158:449–461.

17 Neganova I, Chichagova V, Armstrong L et al. A critical role for p38MAPK signalling pathway during reprogramming of human fibroblasts to iPSCs. *Sci Rep* 2017;7:41693.

18 Neganova I, Shmeleva E, Munkley J et al. JNK/SAPK signaling is essential for efficient reprogramming of human fibroblasts to induced pluripotent stem cells. *STEM CELLS* 2016;34:1198–1212.

19 Ebrahimi B. Reprogramming barriers and enhancers: Strategies to enhance the efficiency and kinetics of induced pluripotency. *Cell Regeneration (London, England)* 2015;4:10.

20 Samavarchi-Tehrani P, Golipour A, David L et al. Functional genomics reveals a BMP-driven mesenchymal-to-epithelial transition in the initiation of somatic cell reprogramming. *Cell Stem Cell* 2010;7:64–77.

21 Hansson J, Rafiee MR, Reiland S et al. Highly coordinated proteome dynamics during reprogramming of somatic cells to pluripotency. *Cell Rep* 2012;2:1579–1592.

22 Benevento M, Tonge PD, Puri MC et al. Proteome adaptation in cell reprogramming proceeds via distinct transcriptional networks. *Nat Commun* 2014;5:5613.

23 Li W, Ding S. Small molecules that modulate embryonic stem cell fate and somatic cell reprogramming. *Trends Pharmacol Sci* 2010;31:36–45.

24 Ichida JK, Blanchard J, Lam K et al. A small-molecule inhibitor of TGF- $\beta$  signaling

replaces Sox2 in reprogramming by inducing Nanog. *Cell Stem Cell* 2009;5:491–503.

25 Karetka MS, Gorges LL, Hafeez S et al. Inhibition of pluripotency networks by the Rb tumor suppressor restricts reprogramming and tumorigenesis. *Cell Stem Cell* 2015;16:39–50.

26 Sudhir PR, Kumari MP, Hsu WT et al. Integrative omics connects N-glycoproteome-wide alterations with pathways and regulatory events in induced pluripotent stem cells. *Sci Rep* 2016;6:36109.

27 Sakurai K, Talukdar I, Patil VS et al. Kinome-wide functional analysis highlights the role of cytoskeletal remodeling in somatic cell reprogramming. *Cell Stem Cell* 2014;14:523–534.

28 Li Z, Rana TM. A kinase inhibitor screen identifies small-molecule enhancers of reprogramming and iPSC cell generation. *Nat Commun* 2012;3:1085.

29 Mah N, Wang Y, Liao MC et al. Molecular insights into reprogramming-initiation events mediated by the OSMK gene regulatory network. *PLoS One* 2011;6:e24351.

30 Spiegel AM, Weinstein LS. Inherited diseases involving G proteins and G protein-coupled receptors. *Annu Rev Med* 2004;55:27–39.

31 Choi HY, Saha SK, Kim K et al. G protein-coupled receptors in stem cell maintenance and somatic reprogramming to pluripotent or cancer stem cells. *BMB Rep* 2015;48:68–80.

32 Nakamura K, Salomonis N, Tomoda K et al. G(i)-coupled GPCR signaling controls the formation and organization of human pluripotent colonies. *PLoS One* 2009;4:e7780.

33 Layden BT, Newman M, Chen F et al. G protein coupled receptors in embryonic stem cells: A role for Gs- $\alpha$  signaling. *PLoS One* 2010;5:e9105.

34 Faherty S, Fitzgerald A, Keohan M et al. Self-renewal and differentiation of mouse embryonic stem cells as measured by Oct4 expression: The role of the cAMP/PKA pathway. *In Vitro Cell Dev Biol Anim* 2007;43:37–47.

35 Pebay A, Bonder CS, Pitson SM. Stem cell regulation by lysophospholipids. *Prostaglandins Other Lipid Mediat* 2007;84:83–97.

36 Pebay A, Wong RC, Pitson SM et al. Essential roles of sphingosine-1-phosphate and platelet-derived growth factor in the maintenance of human embryonic stem cells. *STEM CELLS* 2005;23:1541–1548.

37 Pells S, Koutsouraki E, Morfopoulou S et al. Novel human embryonic stem cell regulators identified by conserved and distinct CpG island methylation state. *PLoS One* 2015;10:e0131102.

38 Sato K, Kon J, Tomura H et al. Activation of phospholipase C-Ca<sup>2+</sup> system by sphingosine 1-phosphate in CHO cells transfected with Edg-3, a putative lipid receptor. *FEBS Lett* 1999;443:25–30.

39 Eastham AM, Spencer H, Soncin F et al. Epithelial-mesenchymal transition events during human embryonic stem cell differentiation. *Cancer Res* 2007;67:11254–11262.

40 Harb N, Archer TK, Sato N. The Rho-Rock-Myosin signaling axis determines cell-cell integrity of self-renewing pluripotent stem cells. *PLoS One* 2008;3:e3001.

41 Ohgushi M, Matsumura M, Eiraku M et al. Molecular pathway and cell state responsible for dissociation-induced apoptosis in human pluripotent stem cells. *Cell Stem Cell* 2010;7:225–239.

42 Nobes CD, Hall A. Rho, Rac, and cdc42 GTPases regulate the assembly of multimolecular focal complexes associated with actin stress fibers, lamellipodia, and filopodia. *Cell* 1995;81:53–62.

43 Ridley AJ. Rho family proteins: Coordinating cell responses. *Trends Cell Biol* 2001;11:471–477.

44 Shan D, Chen L, Wang D et al. The G protein G $\alpha$ (13) is required for growth factor-induced cell migration. *Dev Cell* 2006;10:707–718.

45 Etienne-Manneville S, Hall A. Rho GTPases in cell biology. *Nature* 2002;420:629–635.

46 Sumi T, Matsumoto K, Shibuya A et al. Activation of LIM kinases by myotonic dystrophy kinase-related Cdc42-binding kinase alpha. *J Biol Chem* 2001;276:23092–23096.

47 Toshima J, Toshima JY, Amano T et al. Cofilin phosphorylation by protein kinase testicular protein kinase 1 and its role in integrin-mediated actin reorganization and focal adhesion formation. *Mol Biol Cell* 2001;12:1131–1145.

48 Okamoto H, Takuwa N, Yokomizo T et al. Inhibitory regulation of Rac activation, membrane ruffling, and cell migration by the G protein-coupled sphingosine-1-phosphate receptor EDG5 but not EDG1 or EDG3. *Mol Cell Biol* 2000;20:9247–9261.

49 Vitillo L, Baxter M, Iskender B et al. Integrin-associated focal adhesion kinase protects human embryonic stem cells from apoptosis, detachment, and differentiation. *Stem Cell Rep* 2016;7:167–176.

50 Narva E, Stubb A, Guzman C et al. A strong contractile actin fence and large adhesions direct human pluripotent colony morphology and adhesion. *Stem Cell Rep* 2017;9:67–76.

51 Takahashi K, Yamanaka S. Induction of pluripotent stem cells from mouse embryonic and adult fibroblast cultures by defined factors. *Cell* 2006;126:663–676.

52 Omole AE, Fakoya AOJ. Ten years of progress and promise of induced pluripotent stem cells: Historical origins, characteristics, mechanisms, limitations, and potential applications. *PeerJ* 2018;6:e4370.

53 Ishii I, Ye X, Friedman B et al. Marked perinatal lethality and cellular signaling deficits in mice null for the two sphingosine 1-phosphate (S1P) receptors, S1P(2)/LP(B2)/EDG-5 and S1P(3)/LP(B3)/EDG-3. *J Biol Chem* 2002;277:25152–25159.

54 Walker A, Su H, Conti MA et al. Non-muscle myosin II regulates survival threshold of pluripotent stem cells. *Nat Commun* 2010;1:71.

55 Rosowski KA, Mertz AF, Norcross S et al. Edges of human embryonic stem cell colonies display distinct mechanical properties and differentiation potential. *Sci Rep* 2015;5:14218.

56 Chen G, Hou Z, Gulbranson DR et al. Actin-myosin contractility is responsible for the reduced viability of dissociated human embryonic stem cells. *Cell Stem Cell* 2010;7:240–248.

57 Watanabe K, Ueno M, Kamiya D et al. A ROCK inhibitor permits survival of dissociated

human embryonic stem cells. *Nat Biotechnol* 2007;25:681–686.

**58** Krawetz RJ, Li X, Rancourt DE. Human embryonic stem cells: Caught between a ROCK inhibitor and a hard place. *BioEssays* 2009;31:336–343.

**59** Gerecht S, Bettinger CJ, Zhang Z et al. The effect of actin disrupting agents on

contact guidance of human embryonic stem cells. *Biomaterials* 2007;28:4068–4077.

**60** Li L, Wang BH, Wang S et al. Individual cell movement, asymmetric colony expansion, rho-associated kinase, and E-cadherin impact the clonogenicity of human embryonic stem cells. *Biophys J* 2010;98:2442–2451.

**61** Wadkin LE, Elliot LF, Neganova I et al. Dynamics of single human embryonic stem cells and their pairs: A quantitative analysis. *Sci Rep* 2017;7:570.

**62** Bellis SL, Miller JT, Turner CE. Characterization of tyrosine phosphorylation of paxillin in vitro by focal adhesion kinase. *J Biol Chem* 1995;270:17437–17441.



See [www.StemCells.com](http://www.StemCells.com) for supporting information available online.